

University of Dundee

**Development and characterization of phospho-ubiquitin antibodies to monitor PINK1-PRKN signaling in cells and tissue**

Watzlawik, Jens O.; Hou, Xu; Richardson, Tyrique; Lewicki, Szymon L.; Siuda, Joanna; Wszolek, Zbigniew K.

*Published in:*  
Autophagy

*DOI:*  
[10.1080/15548627.2024.2356490](https://doi.org/10.1080/15548627.2024.2356490)

*Publication date:*  
2024

*Licence:*  
CC BY

*Document Version*  
Publisher's PDF, also known as Version of record

[Link to publication in Discovery Research Portal](#)

*Citation for published version (APA):*

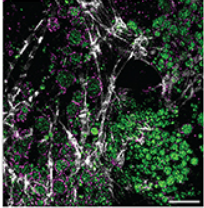
Watzlawik, J. O., Hou, X., Richardson, T., Lewicki, S. L., Siuda, J., Wszolek, Z. K., Cook, C. N., Petrucelli, L., DeTure, M., Dickson, D. W., Antico, O., Muqit, M. M. K., Fishman, J. B., Pirani, K., Kumaran, R., Polinski, N. K., Fiesel, F. C., & Springer, W. (2024). Development and characterization of phospho-ubiquitin antibodies to monitor PINK1-PRKN signaling in cells and tissue. *Autophagy*. Advance online publication. <https://doi.org/10.1080/15548627.2024.2356490>

**General rights**

Copyright and moral rights for the publications made accessible in Discovery Research Portal are retained by the authors and/or other copyright owners and it is a condition of accessing publications that users recognise and abide by the legal requirements associated with these rights.

**Take down policy**

If you believe that this document breaches copyright please contact us providing details, and we will remove access to the work immediately and investigate your claim.



## Development and characterization of phospho-ubiquitin antibodies to monitor PINK1-PRKN signaling in cells and tissue

Jens O. Watzlawik, Xu Hou, Tyrique Richardson, Szymon L. Lewicki, Joanna Siuda, Zbigniew K. Wszolek, Casey N. Cook, Leonard Petrucelli, Michael DeTure, Dennis W. Dickson, Odetta Antico, Miratul M. K. Muqit, Jordan B. Fishman, Karima Pirani, Ravindran Kumaran, Nicole K. Polinski, Fabienne C. Fiesel & Wolfdieter Springer

**To cite this article:** Jens O. Watzlawik, Xu Hou, Tyrique Richardson, Szymon L. Lewicki, Joanna Siuda, Zbigniew K. Wszolek, Casey N. Cook, Leonard Petrucelli, Michael DeTure, Dennis W. Dickson, Odetta Antico, Miratul M. K. Muqit, Jordan B. Fishman, Karima Pirani, Ravindran Kumaran, Nicole K. Polinski, Fabienne C. Fiesel & Wolfdieter Springer (27 May 2024): Development and characterization of phospho-ubiquitin antibodies to monitor PINK1-PRKN signaling in cells and tissue, *Autophagy*, DOI: [10.1080/15548627.2024.2356490](https://doi.org/10.1080/15548627.2024.2356490)

**To link to this article:** <https://doi.org/10.1080/15548627.2024.2356490>



© 2024 The Author(s). Published by Informa UK Limited, trading as Taylor & Francis Group.



[View supplementary material](#)



Published online: 27 May 2024.



[Submit your article to this journal](#)



Article views: 1262







[View related articles](#)



[View Crossmark data](#)

## Development and characterization of phospho-ubiquitin antibodies to monitor PINK1-PRKN signaling in cells and tissue

Jens O. Watzlawik <sup>a,\*</sup>, Xu Hou <sup>a,\*</sup>, Tyrique Richardson<sup>a</sup>, Szymon L. Lewicki<sup>a</sup>, Joanna Siuda<sup>b</sup>, Zbigniew K. Wszolek<sup>c</sup>, Casey N. Cook<sup>a,d</sup>, Leonard Petrucelli<sup>a,d</sup>, Michael DeTure<sup>a</sup>, Dennis W. Dickson<sup>a,d</sup>, Odetta Antico<sup>e</sup>, Miratul M. K. Muqit<sup>e</sup>, Jordan B. Fishman<sup>f</sup>, Karima Pirani<sup>g</sup>, Ravindran Kumaran<sup>h</sup>, Nicole K. Polinski<sup>i</sup>, Fabienne C. Fiesel <sup>a,d</sup>, and Wolfdieter Springer <sup>a,d</sup>

<sup>a</sup>Department of Neuroscience, Mayo Clinic, Jacksonville, FL, USA; <sup>b</sup>Department of Neurology, Faculty of Medical Sciences in Katowice, Medical University of Silesia, Katowice, Poland; <sup>c</sup>Department of Neurology, Mayo Clinic, Jacksonville, FL, USA; <sup>d</sup>Neuroscience PhD Program, Mayo Clinic Graduate School of Biomedical Sciences, Jacksonville, FL, USA; <sup>e</sup>MRC Protein Phosphorylation and Ubiquitylation Unit, School of Life Sciences, University of Dundee, Dundee, UK; <sup>f</sup>21st Century Biochemicals Inc, Marlborough, MA, USA; <sup>g</sup>ImmunoPrecise Antibodies Ltd, Victoria, BC, Canada; <sup>h</sup>Abcam plc, Cambridge, UK; <sup>i</sup>The Michael J. Fox Foundation for Parkinson's Research, New York, NY, USA

### ABSTRACT

The selective removal of dysfunctional mitochondria, a process termed mitophagy, is critical for cellular health and impairments have been linked to aging, Parkinson disease, and other neurodegenerative conditions. A central mitophagy pathway is orchestrated by the ubiquitin (Ub) kinase PINK1 together with the E3 Ub ligase PRKN/Parkin. The decoration of damaged mitochondrial domains with phosphorylated Ub (p-S65-Ub) mediates their elimination through the autophagy system. As such p-S65-Ub has emerged as a highly specific and quantitative marker of mitochondrial damage with significant disease relevance. Existing p-S65-Ub antibodies have been successfully employed as research tools in a range of applications including western blot, immunocytochemistry, immunohistochemistry, and enzyme-linked immunosorbent assay. However, physiological levels of p-S65-Ub in the absence of exogenous stress are very low, therefore difficult to detect and require reliable and ultrasensitive methods. Here we generated and characterized a collection of novel recombinant, rabbit monoclonal p-S65-Ub antibodies with high specificity and affinity in certain applications that allow the field to better understand the molecular mechanisms and disease relevance of PINK1-PRKN signaling. These antibodies may also serve as novel diagnostic or prognostic tools to monitor mitochondrial damage in various clinical and pathological specimens.

**Abbreviations:** AD: Alzheimer disease; CCCP: carbonyl cyanide 3-chlorophenylhydrazone; ELISA: enzyme-linked immunosorbent assay; HEK293E cell: human embryonic kidney E cell; ICC: immunocytochemistry; IHC: immunohistochemistry; KO: knockout; LoB: limit of blank; LoD: limit of detection; LoQ: limit of quantification; MEF: mouse embryonic fibroblast; MSD: Meso Scale Discovery; n.s.: non-significant; nonTg: non-transgenic; PBMC: peripheral blood mononuclear cell; PD: Parkinson disease; p-S65-PRKN: phosphorylated PRKN at serine 65; p-S65-Ub: phosphorylated Ub at serine 65; Ub: ubiquitin; WT: wild-type.

### ARTICLE HISTORY

Received 27 December 2023  
Revised 7 May 2024  
Accepted 13 May 2024

### KEYWORDS

Autophagy; mitochondria; mitophagy; Parkinson disease; PINK1; ubiquitin

### Introduction


Mitophagy is a cytoprotective mechanism for the selective and timely removal of dysfunctional or superfluous mitochondria through autophagy. One central mitophagy mechanism that provides specificity for damaged mitochondria is the phospho-ubiquitination of mitochondrial proteins, which fosters the recruitment of autophagy receptors only to those organelles that need to be degraded [1]. PINK1 (PTEN induced kinase 1) and PRKN (parkin RBR E3 ubiquitin protein ligase) are the key players of this Ub-tagging process and complete loss of either enzyme leads to early-onset Parkinson disease (PD). Upon mitochondrial damage, PINK1 accumulates at the outer mitochondrial membrane bound to the TOMM complex [2,3] where it phosphorylates serine 65 on Ub (p-S65-Ub) that is either free or

already attached to outer mitochondrial proteins as monomer or different types of poly-Ub chains [4–6]. PINK1 also phosphorylates the E3 Ub ligase PRKN at a conserved serine at position 65 within its Ub-like domain [7,8]. Both PRKN phosphorylation and allosteric p-S65-Ub binding fully activates its E3 Ub ligase activity [9–11]. Activated PRKN attaches additional Ub moieties to mitochondrial proteins, which can be further phosphorylated by PINK1 and serve as additional docking stations to recruit even more cytosolic PRKN to mitochondria. This positive feedback loop between PINK1 and PRKN amplifies the extent of p-S65-Ub coating of damaged mitochondria, which drives their elimination via mitophagy.

Given the causal link between the loss of function in PINK1 or PRKN and early-onset PD, mitophagy dysfunction

**CONTACT** Wolfdieter Springer  Springer.Wolfdieter@mayo.edu  Department of Neuroscience; Mayo Clinic, 4500 San Pablo Road, Jacksonville, FL 32224, USA

\*Contributed equally.

 Supplemental data for this article can be accessed online at <https://doi.org/10.1080/15548627.2024.2356490>

© 2024 The Author(s). Published by Informa UK Limited, trading as Taylor & Francis Group.

This is an Open Access article distributed under the terms of the Creative Commons Attribution License (<http://creativecommons.org/licenses/by/4.0/>), which permits unrestricted use, distribution, and reproduction in any medium, provided the original work is properly cited. The terms on which this article has been published allow the posting of the Accepted Manuscript in a repository by the author(s) or with their consent.

has been long considered to play an important role in disease pathogenesis [12]. Mitochondrial impairments are commonly found in aging and age-related diseases including neurodegenerative disorders, and mitophagy defects are likely also widespread [13]. As the joint product of PINK1 and PRKN enzymatic activity, p-S65-Ub can be used as a quantitative measure of mitochondrial health and mitophagy alteration. Absent or reduced p-S65-Ub levels result from failure to properly activate mitophagy in model organisms with *PINK1* or *PRKN* knockout (KO) or mutations [14–16]. In contrast, elevated p-S65-Ub levels can be detected with age and in many diseases and may originate from increased mitochondrial damage or rather may accumulate due to a downstream block of the autophagic-lysosomal degradation system [14,16–18]. p-S65-Ub therefore represents a promising and potent diagnostic marker for damaged mitochondria in cell and animal models as well as in human biofluids and postmortem brain [14,16]. Indeed, p-S65-Ub is currently being tested in several preclinical studies as an early biomarker in different neurodegenerative diseases. However, it should be noted that the overall p-S65-Ub signal in human biofluids at baseline and under pathological conditions is very low and therefore difficult to detect in a reliable manner. Similarly, sensitive histopathological assessment of damaged mitochondria undergoing mitophagy in human brain is still limited and would benefit from reliable tools that are widely available to

further validate injury-prone brain regions and subcellular locations that are positive for the p-S65-Ub signal. In general, the detection of endogenous p-S65-Ub *in vivo* at baseline or under low (chronic) stress is key and requires additional sensitive techniques and antibodies.

To expand the existing repertoire of tools, we here generated and thoroughly characterized a large series of recombinant, rabbit monoclonal antibodies target p-S65-Ub with high specificity (Figure 1). The top performing p-S65-Ub antibody clones for each category were affinity-purified and further interrogated in cells and brain tissue of mouse and human origin and across a range of different applications. While the reference antibody used for comparison is an excellent reagent, some of the top antibody candidates developed herein perform equal to or superior in select applications and are available as a novel resource for the community to study PINK1-PRKN signaling under normal, stress, or disease conditions.

## Results

### Generation and screening of polyclonal rabbit antibodies

Four rabbits were immunized with a combination of N- or C-terminally conjugated p-S65-Ub peptides. Initial bleeds from these animals were tested for immunoreactivity in dot blots

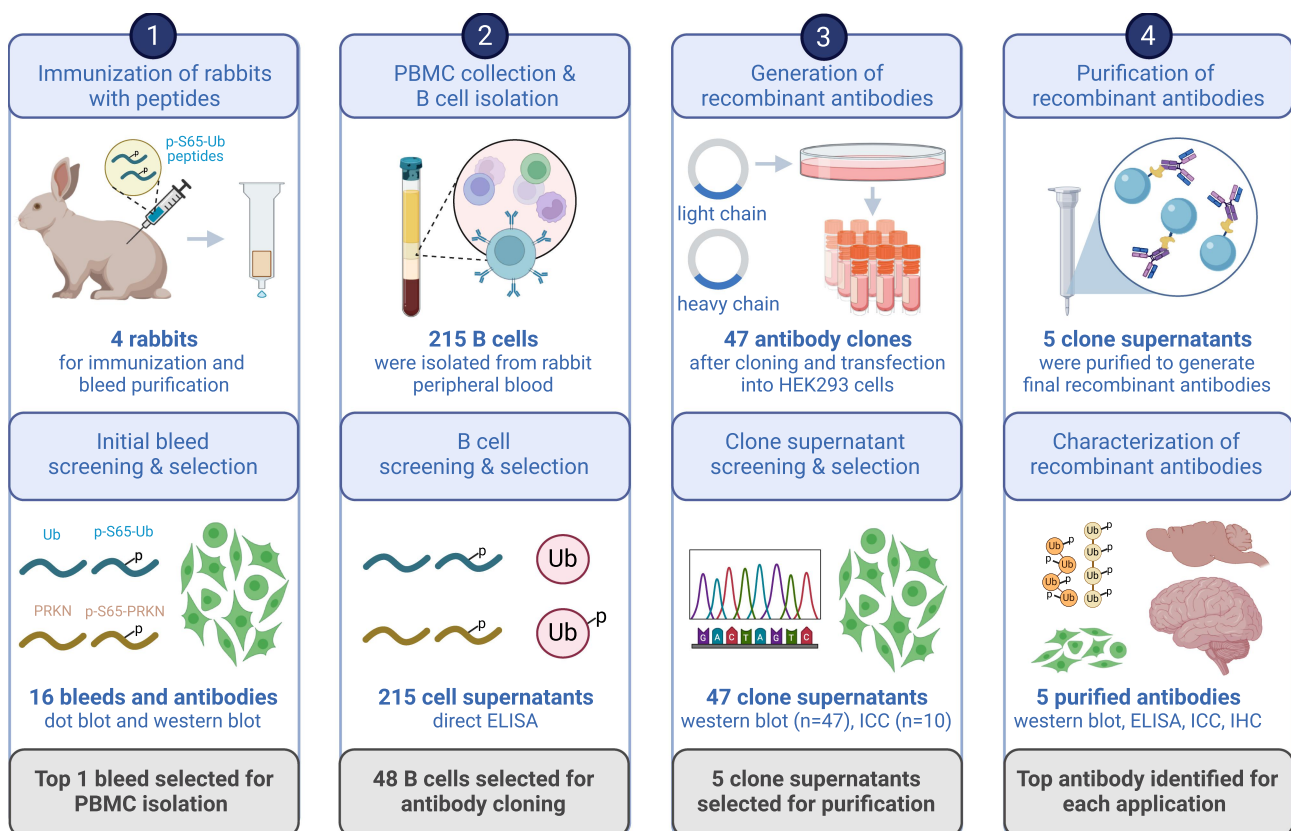


**Figure 1.** Schematic overview of recombinant p-S65-Ub antibody clone generation, selection, and validation. The illustration summarizes the entire process of recombinant, rabbit monoclonal antibody production starting from testing of the initial polyclonal bleeds to the isolation and screening of B cells, and the subsequent cloning of variable heavy and light chain antibody regions into an IgG vector frame. Recombinant antibodies were then sequenced, expressed in HEK293 cells and supernatants were screened by western blot and ICC. The five most promising antibody clones were affinity purified and re-validated by a series of biochemical and imaging analyses using recombinant proteins as well as cells and brain tissues from mouse and human origin. PBMC: peripheral blood mononuclear cell; ELISA: enzyme-linked immunosorbent assay; ICC: immunocytochemistry; IHC: immunohistochemistry. Created with BioRender.com.

toward the respective phosphorylated- and non-phosphorylated Ub and PRKN peptides (Fig. S1A). Based on their stronger immunoreactivity, rabbits (#15021 and #15022) were further selected to receive additional p-S65-Ub peptide booster injections. The resulting affinity-purified polyclonal antibodies were tested in western blots using wild-type (WT) and negative control *PINK1* KO human embryonic kidney (HEK293E) cells that were each treated with the mitochondrial stressor carbonyl cyanide 3-chlorophenylhydrazone (CCCP) (Fig. S1B) [16]. Affinity purified bleeds from rabbit #15022 but not rabbit #15021 demonstrated strong p-S65-Ub immunoreactivity in CCCP-treated WT cells, which was comparable to the commercially available reference antibody. Additional immunodepletion further reduced the nonspecific signal in *PINK1* KO cells. Given the superior signal-to-noise ratio, rabbit #15022 was selected for isolation of peripheral blood mononuclear cells (PBMCs).

### Recombinant monoclonal antibody generation and clonal selection

Collected PBMCs were enriched for antigen-specific B cells, and subsequently diluted for single B cell cultivation. Cell supernatants from a total of 215 single B cell cultures were tested by direct enzyme-linked immunosorbent assay (ELISA) for immunoreactivity toward phosphorylated (serine 65) and non-phosphorylated full-length, monomeric Ub protein as well as non-/phosphorylated Ub and PRKN peptides surrounding the respective serine 65 residues (Table S1). We identified 48 candidates that consisted of 36 B cell cultures producing antibodies that strongly targeted both p-S65-Ub protein and peptide, four with similar specificity but weaker immunoreactivity, four that detected p-S65-Ub protein only but not peptide, and another four that also recognized the corresponding p-S65-PRKN peptide (Table S1). Variable regions of both heavy and kappa chains were subsequently cloned, sequenced, and co-expressed in HEK293 cells to give rise to 47 recombinant IgG antibody clones. A phylogenetic tree was created to determine their clonal relationship (Fig. S2).

We next screened all 47 recombinant clonal supernatants in western blots for affinity and selectivity (Fig. S3). Ten supernatants showed substantially stronger signal with lysates from CCCP-treated WT HEK293E compared to *PINK1* KO cells and were selected for additional validation by immunocytochemistry (ICC). Primary dermal fibroblasts from a PD patient with homozygous *PINK1* Q456X loss-of-function mutation and matching WT cells were left untreated or were challenged with the mitochondrial depolarizer valinomycin and then stained with the top ten clonal supernatants (Fig. S4A). Most supernatants showed only minimal staining in untreated WT cells but detected a robust signal in stressed WT compared to *PINK1* mutant cells. Clones 11H2K3, 29H1K3, 29H2K2, and 30H3K1 had the most intense staining, while two clones showed no real signal increase above background levels (Fig. S4B).

Taken together and considering different biochemical and ICC validation criteria, cell supernatants from five recombinant p-S65-Ub clones (11H2K3, 19H1K1, 29H2K2, 30H3K1, and 41H1K3) were selected for subsequent affinity purification and further detailed characterization.

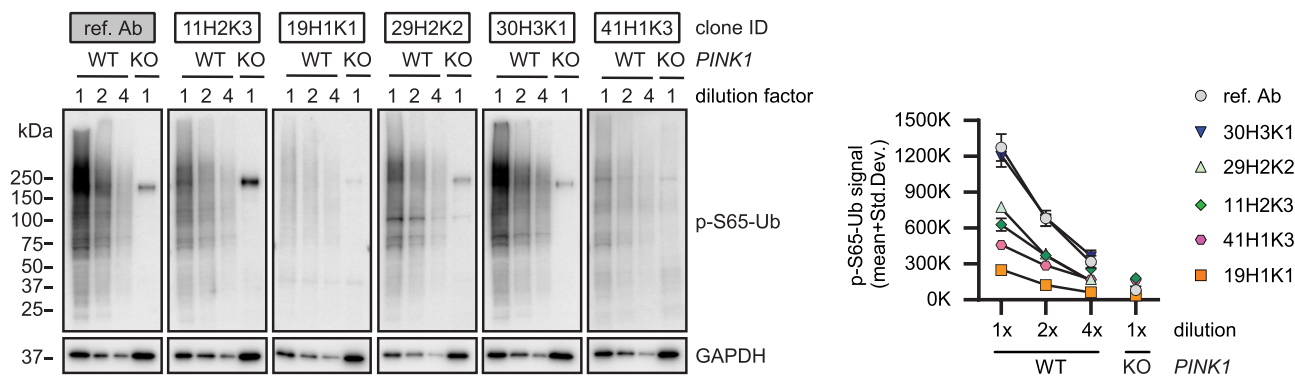
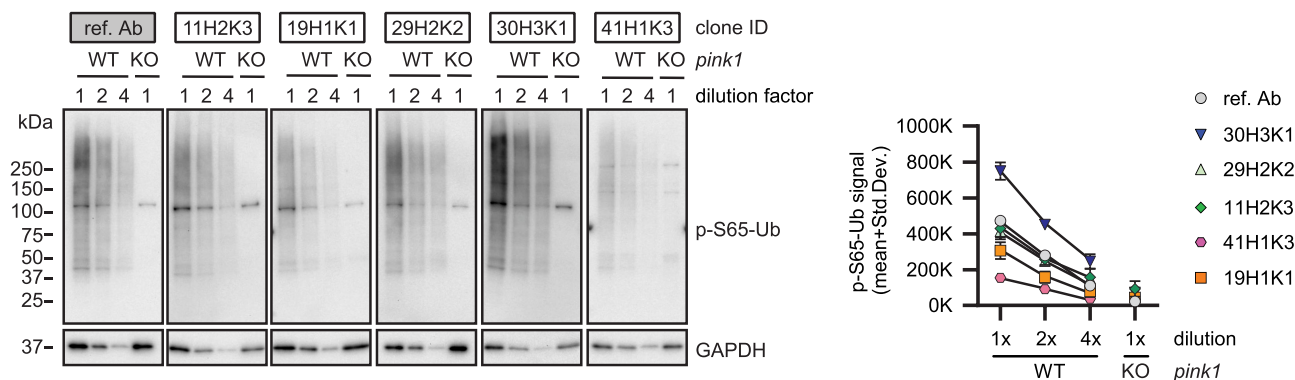
### Western blot assessment of the top affinity purified recombinant p-S65-Ub antibodies

Supernatant from the five top p-S65-Ub clones were next affinity-purified and first re-validated to confirm the previous outcome before expanding to additional analyses. Briefly, WT and *PINK1* KO HEK293E cells (Figure 2A) as well as WT and *pink1* KO mouse embryonic fibroblasts (MEFs) (Figure 2B) were treated with mitochondrial stressors and their lysates were analyzed by western blot. All recombinant affinity-purified p-S65-Ub antibodies were used in identical concentration, except the reference antibody, which was used five times diluted. All antibodies gave increased signal in WT but not the corresponding *PINK1/pink1* KO cells of human and mouse origin (Figure 2A, B). In WT HEK293E cells, the reference antibody and clone 30H3K1 were able to detect p-S65-Ub with highest intensity, followed by clones 29H2K2 and 11H2K3 and subsequently clones 19H1K1 and 41H1K3. Similar to the outcome in HEK293 cells, clone 30H3K1 outperformed the other four recombinant clones also in MEF cells. Clones 29H2K2 and 11H2K3 followed on next places and lastly clones 19H1K1 and 41H1K3. Different from HEK293 cells, in MEF cells the reference antibody (while at the same time 5-fold more diluted) targeted its antigen with ~2-fold lower intensity compared to clone 30H3K1. If we assume a linear signal-concentration range, then the reference antibody is still performing better than clone 30H3K1. Overall, the reference antibody followed by clone 30H3K1 performed the best in western blot while all five affinity-purified clones plus reference antibody showed very little background signal in human and mouse *PINK1/pink1* KO cells treated with mitochondrial stressors, suggesting high specificity.

### Testing antibodies with recombinant p-S65-Ub chains using sandwich ELISAs

We next tested the purified recombinant p-S65-Ub antibodies in a sandwich ELISA format on a Meso Scale Discovery (MSD) platform. Rabbit p-S65-Ub antibodies were used as capturing agents and combined with a mouse total Ub antibody (P4D1) as detecting reagent as published previously [16]. We first tested recombinant p-S65-Ub tetramers with K48 or K63 chain linkage, the two most abundant Ub chain types in cells, and used their non-phosphorylated counterparts as negative controls and determined the Limit of Blank (LoB), the Limit of Detection (LoD), and the Limit of Quantification (LoQ) according to *Armbruster and Pry (2008)* [19] (Table 1; Figure 3A). The LoB represents the relative noise or background, and was relatively high for clones 41H1K3, 11H2K3, and 29H2K2. The LoD was similar compared to the corresponding LoB and consequently also relatively high for the same clones mentioned (41H1K3, 11H2K3, and 29H2K2). Importantly, the LoQ for K48-linked p-S65-Ub tetramers was lowest for clone 19H1K1 at 100 fg/ml, which was even lower compared to the reference antibody.

Of note, the LoQs for K63-linked p-S65-Ub tetramers were in most cases substantially higher compared to those for K48-linked p-S65-Ub tetramers, which is in line with

**A HEK293E cells plus CCCP****B MEF cells plus valinomycin**

**Figure 2.** Western blot assessment of the selected affinity-purified p-S65-Ub antibodies in cells. (A) HEK293E cells and (B) mouse embryonic fibroblasts with (WT) or without PINK1 expression (*PINK1* KO or *pink1* KO) were treated with mitochondrial depolarizer. All western blots were run and developed side-by-side. Representative western blot from three total replicates are shown for the top five p-S65-Ub antibody clones in each cell type plus reference antibody. Note that concentrations of the tested p-S65-Ub antibodies are five times higher compared to the reference antibody. For both WT HEK293 cells and WT MEFs, we used different dilutions of the WT lysates, namely 30 (1× diluted), 15 (2× diluted) and 7.5 μg (4× diluted) for WT HEK293 cells plus 30 μg of *PINK1* KO HEK293 cells (1× diluted) respective 10 (1× diluted), 5 (2× diluted), 2.5 μg (4× diluted) total protein for WT MEFs and 10 μg for *pink1* KO MEFs (1× diluted). GAPDH was used as loading control. A densitometric quantification of p-S65-Ub raw data is shown for all antibodies in both cell types with the entire lane being quantified (instead of a single band). KO: knockout; ref. Ab: reference antibody; WT: wild-type.

**Table 1.** LoB, LoD, and LoQ of p-S65-Ub MSD ELISA with recombinant protein.

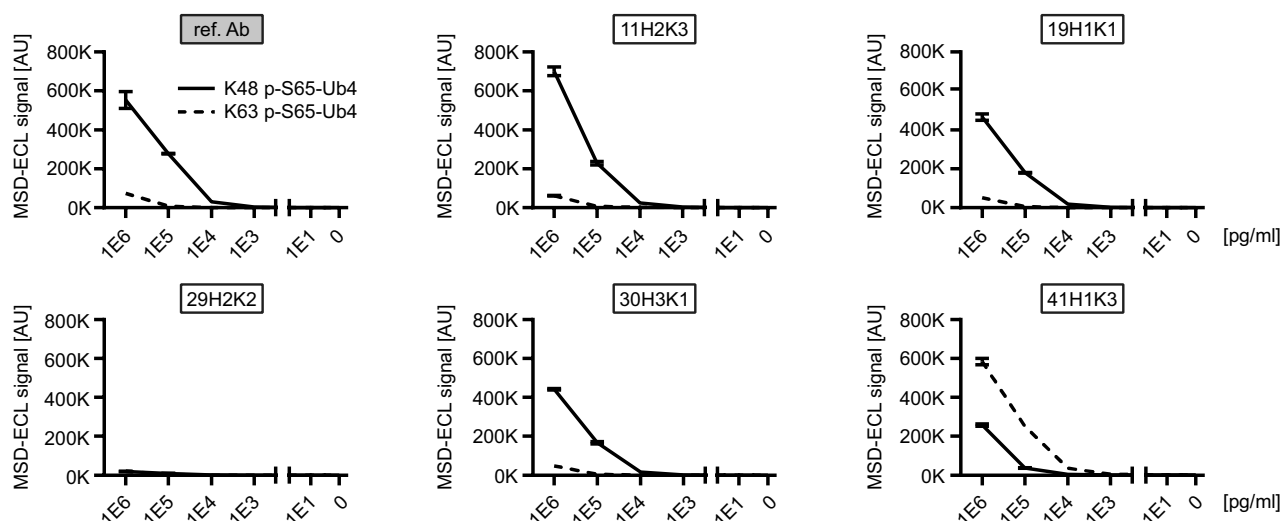
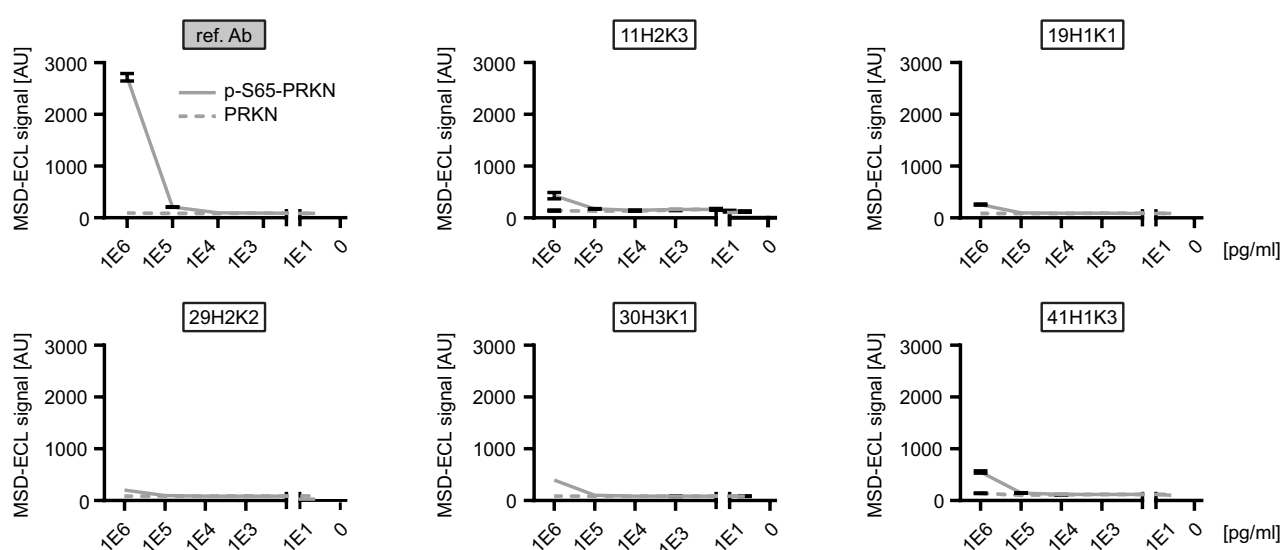
	ref. Ab	11H2K3	19H1K1	29H2K2	30H3K1	41H1K3
LoB (MSD-ECL [AU])	469	1162	522	774	578	2340
LoD for K48 p-S65-Ub4 (MSD-ECL [AU])	472	1268	538	860	590	2454
LoD for K63 p-S65-Ub4 (MSD-ECL [AU])	473	1178	522	804	912	2349
LoQ for K48 p-S65-Ub4 (fg/ml)	1×10 <sup>4</sup>	1×10 <sup>6</sup>	100	1×10 <sup>7</sup>	1×10 <sup>5</sup>	1×10 <sup>6</sup>
LoQ for K63 p-S65-Ub4 (fg/ml)	1×10 <sup>6</sup>	1×10 <sup>7</sup>	1×10 <sup>6</sup>	1×10 <sup>7</sup>	1×10 <sup>7</sup>	1×10 <sup>5</sup>
Chain preference	K48 >> K63	K48 >> K63	K48 >> K63	K48 = K63	K48 >> K63	K48 << K63

ref.Ab – reference antibody, LoB – Limit of Blank, LoD – Limit of Detection, LoQ – Limit of Quantitation, Ub – ubiquitin tetramer, K48 - polyubiquitin chain linked by lysine residue 48, K63 - polyubiquitin chain linked by lysine residue 63.

previously published results [16]. Two exceptions were clones 41H1K3 and 29H2K2. Remarkably, clone 41H1K3 had a stronger preference toward Ub tetramers with K63-linkage relative to those with K48-linkage, which is reflected in a 10-fold lower LoQ for K63-linkage compared to Ub chains of the K48-linkage type. In contrast, the LoQ for both K48 and K63-linked p-S65-Ub were both similarly high (10 ng/ml each) for clone 29H2K2 suggesting that this antibody may not be the best option for ELISA-based detection (Table 1; Figure 3A). The range of linearity in this assay differed between p-S65-Ub species used and was between 10

ng/ml and 1 μg/ml for K63 p-S65-Ub tetramers and between 1 ng/ml and 1 μg/ml for K48 p-S65-Ub tetramers. The coefficient of variation was excellent for all clones and matrices analyzed and was always well below 10% (data not shown).

Given the sequence similarity of phosphorylated epitopes around serine 65 in both Ub versus PRKN, we tested all purified recombinant antibodies toward phosphorylated and non-phosphorylated PRKN protein in a direct ELISA on an MSD platform (Figure 3B). It is noteworthy that all antibodies including the reference antibody showed no cross-reactivity toward p-S65-PRKN or total PRKN except for the highest

**A Sandwich ELISA: Recombinant p-S65-Ub tetramers****B Direct ELISA: Recombinant p-S65-PRKN/PRKN protein**

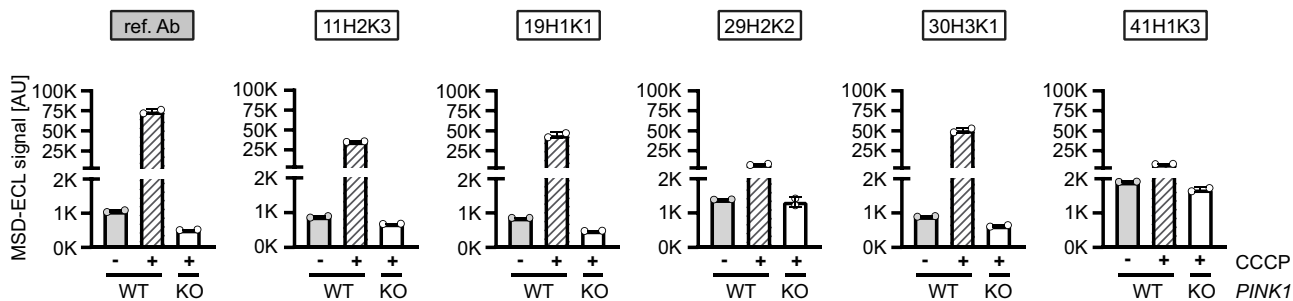
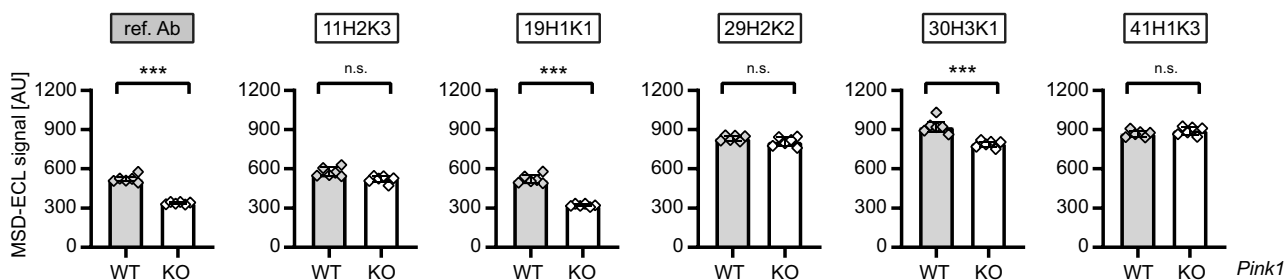
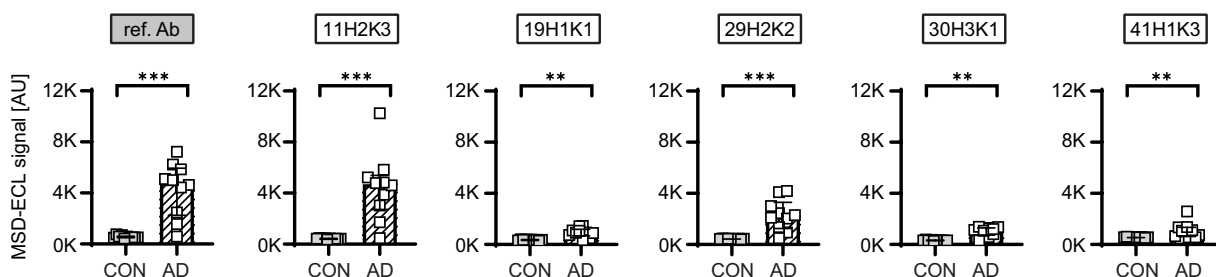
**Figure 3.** Assessing the top p-S65-Ub antibodies in ELISA using recombinant protein. (A) Sandwich ELISA results for the detection of recombinant K48 (solid line) and K63 (dash line) p-S65-Ub tetramers (Ub4) that were serially diluted to the range of 1–1,000,000 pg/ml. (B) Direct ELISA results for the detection of p-S65-PRKN and nonphosphorylated PRKN recombinant proteins that were serially diluted to the range of 1–1,000,000 pg/ml.  $N=2$ . Data are shown as mean with SD. ref. Ab: reference antibody.

concentration tested (1  $\mu$ g/ml). At this concentration, equimolar amounts of p-S65-Ub monomer resulted in almost 600-fold higher MSD-ECL signal for the reference antibody and between 2600 to 6600-fold higher MSD-ECL signal for all other recombinant p-S65-Ub clones. Lack of significant cross-reactivity with recombinant p-S65-PRKN protein was further confirmed by western blots (data not shown).

### ELISA-based p-S65-Ub detection in cells and in mouse and human brain lysates

We next tested the purified p-S65-Ub antibodies for ELISA using cell culture lysates (Figure 4A). We used WT and *PINK1* KO HEK293E cells treated with CCCP for 24 h and compared to vehicle (DMSO)-treated WT cells. It is of note

that all antibodies except clone 29H2K2 were able to show differences in p-S65-Ub levels at baseline condition between DMSO-treated WT and CCCP-treated *PINK1* KO cells. In line with previous results using recombinant p-S65-Ub chains, clone 19H1K1 and the reference p-S65-Ub antibody showed most sensitive p-S65-Ub detection and comparable results for both baseline (1.8- vs. 2.1-fold increases compared DMSO-treated WT to CCCP-treated *PINK1* KO cells) and upon stress (91- vs. 144-fold increases compared CCCP-treated WT over CCCP-treated *PINK1* KO cells) (Figure 4A; Table 2). Interestingly, clone 41H1K3 that showed a higher sensitivity for recombinant K63- over K48-linked p-S65-Ub chains showed the lowest fold changes for p-S65-Ub detection in the cell samples, both at baseline and under mitochondrial stress (Table 2).

**A HEK293E cells****B Mouse hemibrain lysates****C Human frontal cortex brain lysates**

**Figure 4.** Assessing the top p-S65-Ub antibodies by sandwich ELISA using lysates from cells, mouse brain, and human brain. (A) ELISA detection of p-S65-Ub levels in cell lysates from CCCP or DMSO treated WT and *PINK1* KO HEK293E cells. One-way ANOVA.  $N = 2$ . Data are shown as mean with SEM. (B) ELISA detection of p-S65-Ub levels in hemibrain lysates from unstimulated WT and *pink1* KO mice. Unpaired t-test.  $N = 6$  per group. Data are shown as mean with SEM. (C) ELISA detection of p-S65-Ub levels in human brain lysates from neurological normal controls and AD cases. Mann-Whitney U test.  $N = 10$  per group. Data are shown as median with interquartile range. \*  $p < 0.05$ , \*\*  $p < 0.005$ , \*\*\*  $p < 0.0001$ . Asterisks (\*) indicate the comparison to the untreated WT or the comparison between two groups under the brackets. ref. Ab: reference antibody; AD: Alzheimer disease; CON: controls; KO: knockout; n.s.: non-significant; WT: wild-type.

**Table 2.** Comparison of MSD ELISA detection of p-S65-Ub with different testing materials.

Fold change in MSD ELISA detection $\pm$ range	ref. Ab	11H2K3	19H1K1	29H2K2	30H3K1	41H1K3
HEK293E cell baseline detection* (WT vs. <i>PINK1</i> KO)	2.1 $\pm$ 0.02	1.3 $\pm$ 0.03	1.8 $\pm$ 0.01	1.1 $\pm$ 0.04	1.4 $\pm$ 0.1	1.1 $\pm$ 0.07
HEK293E cell stressed condition* (WT vs. <i>PINK1</i> KO)	143.5 $\pm$ 5.9	52 $\pm$ 0.6	91.2 $\pm$ 5.7	5.6 $\pm$ 1.1	80.2 $\pm$ 6.7	4.8 $\pm$ 0.2
Mouse brain baseline detection* (WT vs. <i>pink1</i> KO)	1.5 $\pm$ 0.3	1.1 $\pm$ 0.1	1.6 $\pm$ 0.2	1.0 $\pm$ 0.1	1.2 $\pm$ 0.1	1.0 $\pm$ 0.1
Human brain disease condition <sup>#</sup> (AD vs. control)	9.3 $\pm$ 0.9	10.8 $\pm$ 0.5	2.6 $\pm$ 0.2	4.9 $\pm$ 0.3	3.7 $\pm$ 0.2	2.0 $\pm$ 0.1

\* = ratio of the means is used for cells and mouse tissue, <sup>#</sup> = ratio of the medians is used for human tissue. AD – Alzheimer disease, KO – knockout, ref. Ab – reference antibody, WT – wild-type.

We then tested the performance of recombinant p-S65-Ub antibodies in mouse hemibrain lysates from unstimulated WT and *pink1* KO mice (Figure 4B). As seen with recombinant Ub chains and in cells, clone 19H1K1 and the reference p-S65-Ub antibody again showed comparable results in mouse brains. Both antibodies were able to distinguish between the two genotypes with identical fold changes (1.6) (Table 2). A weaker detection of p-S65-Ub in unstimulated WT mice was found when using clone 30H3K1, while none of the remaining antibodies showed differences in p-S65-Ub levels between WT and *pink1* KO mice (Figure 4B; Table 2).

Finally, we tested the performance of purified p-S65-Ub clones in human autopsy brain lysates from the frontal cortex of Alzheimer disease (AD) cases compared to sex- and age-matched neurologically normal controls (Figure 4C). Different from the results with mouse brain lysates, all p-S65-Ub clones detected significant increases of p-S65-Ub levels in AD cases compared to controls. The highest fold change between the two groups were obtained with clone 11H2K3 (10.8-fold) and the reference antibody (9.3-fold), followed by clones 29H2K2 and 30H3K1 and finally clones 19H1K1 and 41H1K3 (Figure 4C; Table 2). It should be noted that the



reference antibody, clones 19H1K1 and 30H3K1 showed the largest differences between control tissue and the buffer blank (data not shown), suggesting a greater assay window with potentially better detectability of low p-S65-Ub amounts.

### Characterization of p-S65-Ub clones via immunocytochemistry in *PINK1* patient fibroblasts

To further confirm the specificity and sensitivity of the top five p-S65-Ub clones in other applications, we next validated them by ICC in WT and homozygous *PINK1* loss-of-function mutation (*PINK1*<sup>Q456X</sup>) skin fibroblasts. For this, both WT and *PINK1* mutant fibroblasts were left untreated or were treated with the mitochondrial stressor valinomycin, stained with each of the antibodies using the same concentration and measured by high content imaging (Figure 5). Both unstressed WT cells and stressed *PINK1* mutant cells were expected to show minimal p-S65-Ub signal and served as negative controls. Valinomycin-induced mitophagy led to a significant elevation of p-S65-Ub signal in WT fibroblasts as confirmed by the previously validated reference antibody [16] (Figure 5A). All five clones also showed robust immunostaining of treated WT cells but only minimal immunopositive signals in untreated cells or treated *PINK1* mutant cells (Figure 5A), indicating excellent specificity toward p-S65-Ub detection. In the treated WT cells, the highest signal was observed with antibody clones 30H3K1, 11H2K3, and 29H2K2. Clone 19H1K1 showed a moderate intensity, and 41H1K3 resulted in the lowest signal (Figure 5B). The performance of the top three clones was comparable to the reference antibody. The specificity of the antibodies was further confirmed by the strong colocalization of p-S65-Ub-positive signals with the mitochondrial marker HSP60 upon mitochondrial stress in WT cells (Figure 5C).

### Immunohistological assessment of p-S65-Ub clones in transgenic mouse and human AD brain

In addition to ICC in cultured fibroblasts, we next assessed p-S65-Ub labeling in serial hippocampal sections of transgenic mice overexpressing human MAPT/tau protein (rTg4510 mice) (Figure 6 and Fig. S5). We have shown previously that p-S65-Ub is robustly induced in this tauopathy model and can be reliably detected by both immunohistochemistry (IHC) and MSD-ELISA [15,16,18]. Given that the reference antibody performs poorly in IHC [16], the five p-S65-Ub recombinant antibodies were compared with a previously validated in-house p-S65-Ub antibody [14,17] (Figure 6A and Fig. S5). Non-transgenic (nonTg) littermates were used as controls. Typical, punctate p-S65-Ub immunopositive structures (dark brown) were detected by all p-S65-Ub clones at identical concentrations with high specificity in serial brain sections from the 9-month-old transgenic mouse (Figure 6A) but not from nonTg animal (Fig. S5). However, intensity levels were quite different for different recombinant clones and p-S65-Ub-positive structures were most prominently detected with clone 41H1K3 followed by our in-house antibody [14,17,18], and minimal signal was found with the reference antibody (Figure 6A). The performance of clone 41H1K3 was further

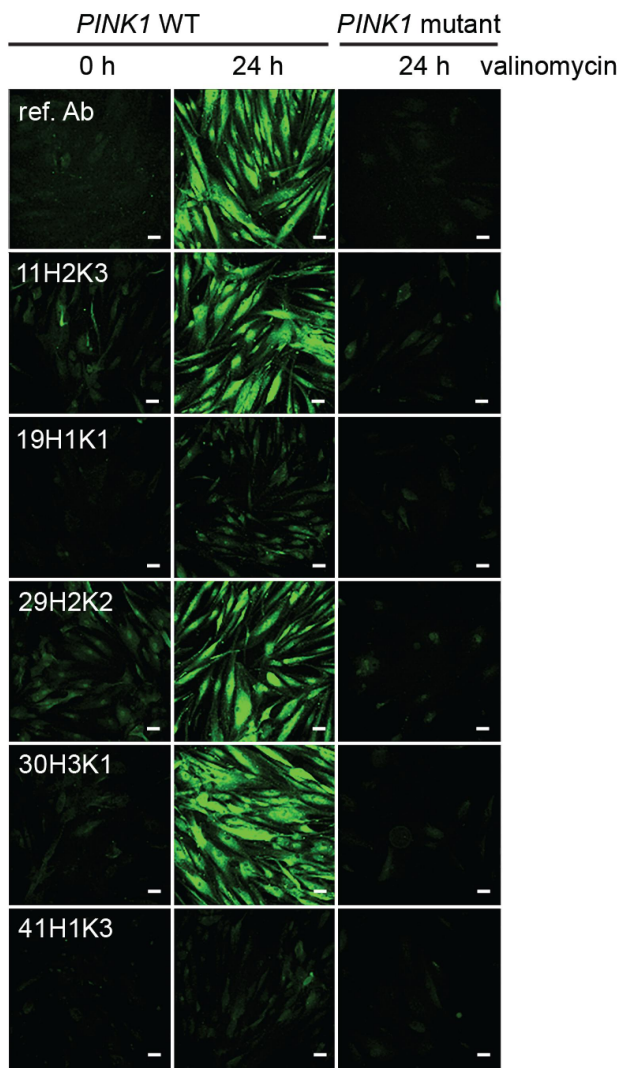
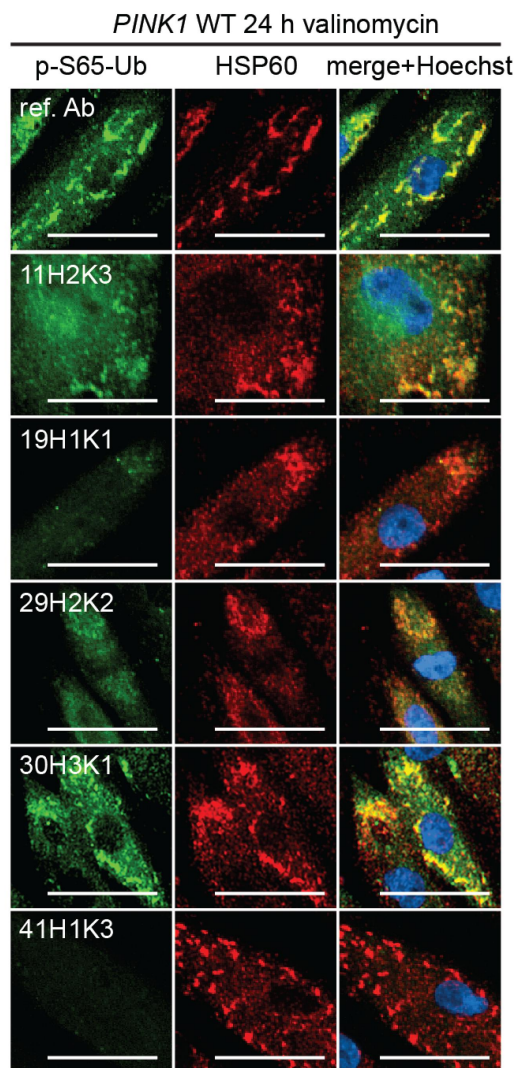
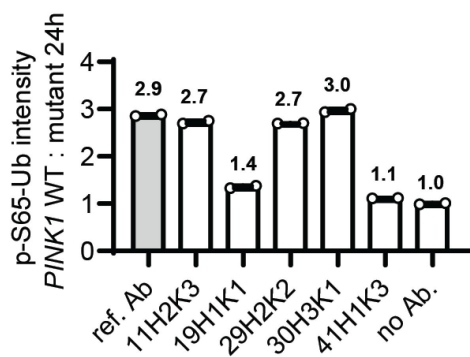
validated in brain sections from three independent rTg4510 mice, in all of which it strongly and consistently detected the respective p-S65-Ub structures (Figure 6B).

Next, we tested the antibody clones on hippocampal regions of human AD brain (Figure 7) [18]. Again, we used the same concentration (0.78 µg/ml) for all tested antibodies to directly compare the sensitivity in serial hippocampal sections (Figure 7A). As previously reported, the in-house antibody detects small granular, cytoplasmic p-S65-Ub immunopositive structures in the AD hippocampus [18]. Similar p-S65-Ub structures were also observed when stained with clones 19H1K1, 29H2K2, and 41H1K3 with lower, similar, or higher signal intensity compared to the in-house antibody, respectively. In contrast to the abovementioned three clones, clone 11H2K3 showed undefined and rather diffuse cytoplasmic staining that has not been previously observed and only very minimal immunoreactive signal was found in clone 30H3K1-stained section. Because of the sensitivity of 41H1K3 we diluted this antibody further and were still able to clearly label p-S65-Ub-positive granules at a much lower concentration of 0.125 µg/ml (Figure 7B). To further confirm the performance of clone 41H1K3, we stained additional slides from three AD brains and again found strong and consistent labeling of p-S65-Ub-positive structures in all cases (Figure 7B).

Taken together, selected clones showed great sensitivity for p-S65-Ub detection in immunostaining in fibroblasts (clones 11H2K3, 29H2K2, and 30H3K1) and brain tissue (clone 41H1K3). While similar characteristic morphologies were detected upon mitochondrial stress in cells, in tauopathy mouse brain, and in human disease autopsy brain, the clones that worked the best for immunostaining in cells and tissue did not appear to overlap.

## Discussion

We here developed and thoroughly characterized a new series of recombinant, rabbit monoclonal antibodies targeting the mitophagy tag p-S65-Ub. Starting from an immunization of four animals, we screened over 200 B cell lines by direct ELISA and cloned and sequenced 47 recombinant antibodies that were further evaluated. The top five clones were affinity purified and their sensitivity and specificity were validated using a range of biochemical and imaging techniques with recombinant Ub chains, gene-edited cells, and patient fibroblasts as well as mouse and human brain tissue. We compared their respective signal-to-noise ratios in samples with diverse complexity and levels of the mitophagy tag at baseline and upon acute, mitochondrial stress or in chronic, diseased conditions, and across applications. It should be noted that the reference antibody overall is an excellent reagent across many different sample types and applications. However, some of the new p-S65-Ub clones showed similar performance, if not slightly better, in selected categories such as ELISA (for mouse brain lysates) and ICC or were superior in IHC compared to the reference antibody. These recombinant antibodies are now available to the community, expanding the toolkit to monitor PINK1-PRKN signaling in different sample types and with different methods (see Table 3 for a summary).

**A Human dermal fibroblasts****C****B**

**Figure 5.** Comparison of the top p-S65-Ub antibodies using ICC of human dermal fibroblasts. All five p-S65-Ub recombinant antibodies and the reference antibody were evaluated by ICC in human primary dermal fibroblasts treated with 2  $\mu$ M valinomycin for 0 or 24 h. All antibodies were used at 1  $\mu$ g/ml. (A) Representative images of p-S65-Ub immunoreactive signals (green) in fibroblasts carrying WT or homozygous *PINK1*<sup>Q456X</sup> mutation. (B) Fluorescence intensities of each antibody was quantified by high content imaging and compared signals from treated WT to the signals from the corresponding *PINK1* mutant fibroblasts. Fold changes are labeled at top of each bar. Samples stained without primary antibody was used a negative control (no Ab). *N* = 2. Data are shown as mean with SEM. (C) Representative zoom-in images of p-S65-Ub and HSP60 immunoreactive signals in treated WT fibroblasts. 24 h of valinomycin treatment induced mitochondrial aggregation (HSP60, red) and the accumulation of p-S65-Ub (green). Nuclei were stained with Hoechst (blue). Scale bar: 50  $\mu$ m. ref. Ab: reference antibody; WT: wild-type.

## MAPT/tau transgenic mouse brain - hippocampus

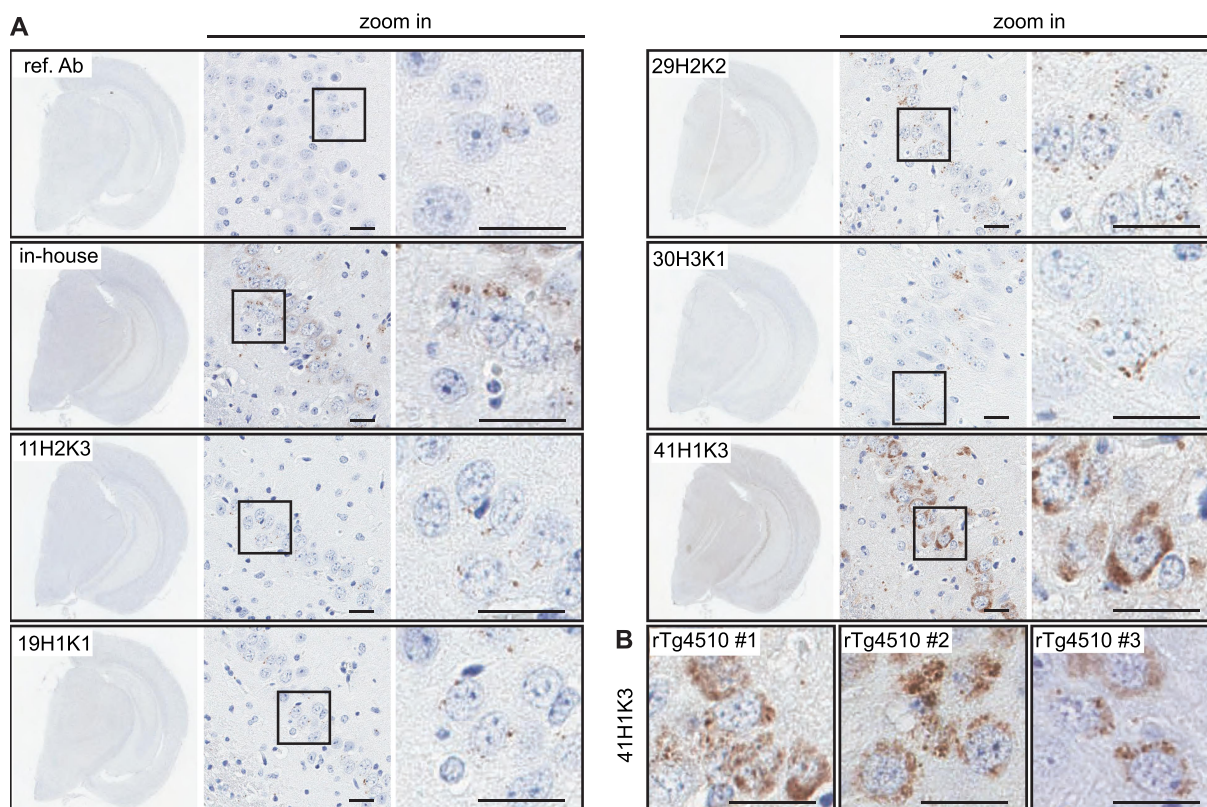


**Figure 6.** Characterization of the top p-S65-Ub antibodies by IHC staining of mouse brain. (A) All five p-S65-Ub recombinant antibodies together with our in-house p-S65-Ub antibody and the reference antibody were evaluated by IHC in serial brain sections from a 9-month-old rTg4510 mouse. Same concentration (1.56 µg/ml) was used for all antibodies. The entire region of the stained hemibrain is shown to the left at 1.5× magnification. Zoom-in images of the highlighted hippocampal regions are shown to the right. Typical punctate p-S65-Ub immunopositive structures (dark brown) were detected by all clones but with different intensity. (B) Brain sections from three different rTg4510 mice were stained with clone 41H1K3 and showed consistent immunostaining pattern. Scale bar: 50 µm. ref. Ab: reference antibody.

Since its discovery [4–6], p-S65-Ub has been recognized as a highly specific and quantitative mitochondrial damage marker of disease relevance [17,20,21]. By now p-S65-Ub has been employed for larger-scale, functional and genetic screening of mitophagy modifiers in cell culture [22,23] and in human autopsy brain [24]. p-S65-Ub can also be detected in clinical samples and may be useful as a biomarker of mitochondrial health and function [16,25]. Yet, physiological levels of p-S65-Ub can vary between different cells and tissues and the normal range of the p-S65-Ub signal needs to be established for each case and sample type. While p-S65-Ub is strongly elevated with stress, age, and various disease conditions in cell and animal models and in humans [14–16,18,26], the underlying causes may differ. It is of note that while p-S65-Ub is a direct result of PINK1 and PRKN enzymatic activities, this mitophagy label is only transitory and highly dynamic in nature as damaged labeled mitochondria are rapidly degraded under healthy, physiological conditions. Greater levels of p-S65-Ub can result from primarily increased mitochondrial stress and damage or from an impaired turnover and reduced flux through the autophagy-lysosome system. Monitoring p-S65-Ub levels over time may allow to better determine mitophagic flux and could help discriminate between both scenarios. Therefore, it may be useful not only as a diagnostic and prognostic

tool, but also as pharmacodynamic and therapeutic biomarker.

Although mitochondrial proteins are the primary targets of p-S65-Ub, the exact nature and composition of the phosphorylated Ub chains is not well understood but could have important implications for outcomes and detection of the signal. A preference for phosphorylation of multi-mono-Ub moieties or short poly-Ub chains has been suggested in cell lines [27], but an increase particularly in K63-linked poly-Ub chains has been noted on mitochondria and appears to be the preferred mitophagy signal in neurons [28,29]. The temporal order of events as well as a certain stoichiometry of the p-S65-Ub signal could also be important for proper induction and flux of mitophagy. As such p-S65-Ub specific antibodies that are also able to better discriminate between different Ub linkages might be particularly useful to further resolve the mitophagy signal *in vivo*. In that regard it is worth noting that some of the clones developed herein seemed to have somewhat distinct chain linkage preferences. While most antibodies to date including clones 11H2K3, 19H1K1, and 30H3K1, seem to have a higher affinity toward recombinant K48-linked p-S65-Ub chains, clone 41H1K3 preferred phosphorylated K63-linked chains. Clone 29H2K2 seemed to recognize both types equally well. Certainly, much more work is needed to fully characterize the binding profiles and

## human Alzheimer disease brain - hippocampus

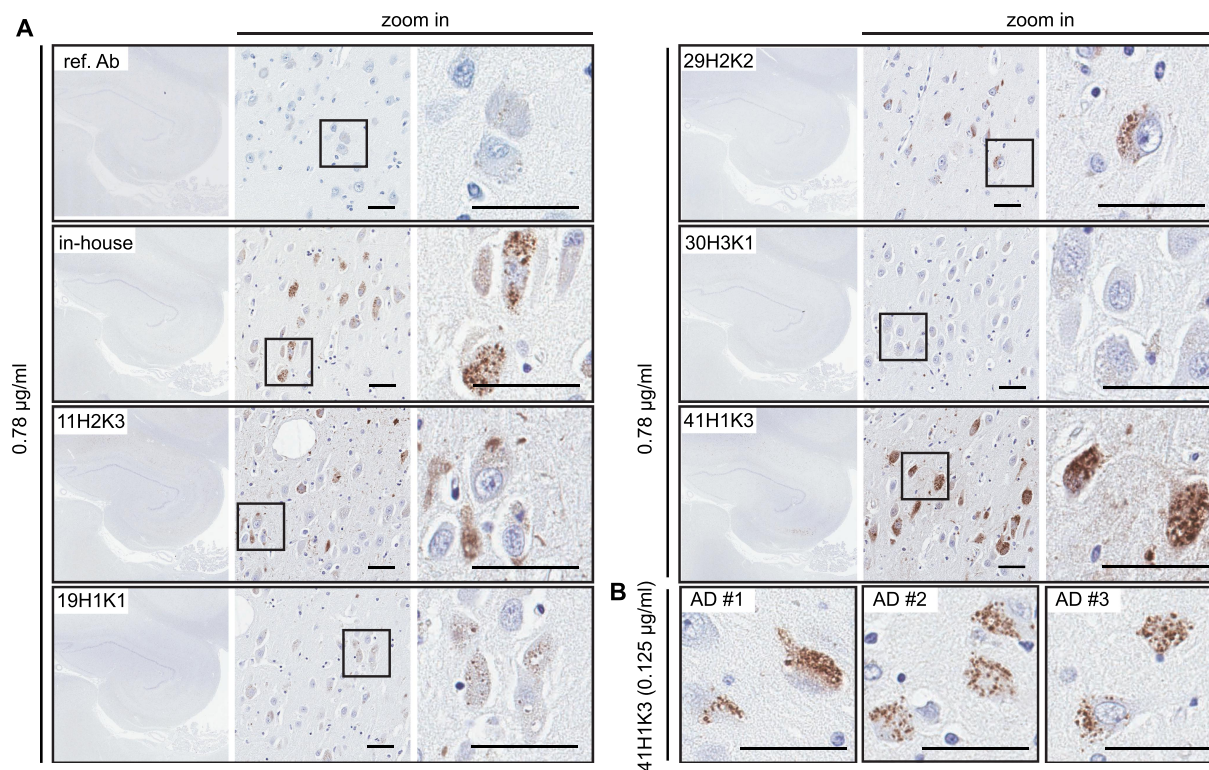


**Figure 7.** Characterization of the top p-S65-Ub antibodies by IHC staining of Alzheimer disease brain. (A) All five p-S65-Ub recombinant antibodies together with our in-house p-S65-Ub antibody and the reference antibody were evaluated by IHC of serial hippocampal sections from Alzheimer disease brain. Same concentration (0.78 µg/ml) was used for all antibodies. The entire stained hippocampal region is shown to the left at 1.5× magnification. Zoom-in images of the highlighted regions are shown to the right. Typical punctate p-S65-Ub immunopositive structures (dark brown) were detected by most of the antibodies at different sensitivity. (B) Hippocampal sections from three different Alzheimer disease cases were stained with 41H1K3 and showed consistent immunostaining pattern. The superior sensitivity of 41H1K3 allowed detection of p-S65-Ub at a much lower concentration (0.125 µg/ml) compared to other antibodies. Scale bar: 50 µm. AD: Alzheimer disease; ref. Ab: reference antibody.

**Table 3.** Commercial p-S65-Ub antibodies for different applications.

Matrix	Cells			Brain tissue	
	WB	ELISA	ICC	ELISA	IHC
human	ref. Ab <sup>#</sup>	ref. Ab <sup>#</sup>	30H3K1 <sup>#,*</sup>	ref. Ab <sup>#</sup>	41H1K3 <sup>#,*</sup>
	30H3K1*	30H3K1*	ref. Ab	30H3K1*	
	41H1K3	19H1K1		19H1K1	
mouse	ref. Ab <sup>#</sup>			19H1K1 <sup>#,*</sup>	41H1K3 <sup>#,*</sup>
	30H3K1*	NT	NT	ref. Ab	
	19H1K1			30H3K1	

<sup>#</sup>= denotes best overall antibody for the application in that sample type, \* = denotes best new recombinant clone for the application in that sample type. WB – western blot, ICC – immunocytochemistry, IHC – immunohistochemistry, ref. Ab – reference antibody, NT – not yet tested.

determine selectivity and affinity of the antibody clones, but a toolkit consisting of clones with differential binding abilities combined with sophisticated mass spectrometry approaches [30] may provide a unique opportunity to decode the complexity of the p-S65-Ub signal in health and disease.

We interrogated the top five antibodies across a range of methods using cell and brain tissue samples of mouse and human origin alongside with appropriate controls for each setting. It is noteworthy that none of the top five clones performed best in all tested applications or with all sample types. Instead, 30H3K1, 19H1K1, and 41H1K3 were selected

as the best clones for different applications and are currently in production for public access (see details in Materials and Methods). Clone 30H3K1 convinced particularly through its performance in western blots and ICC, clone 41H1K3 showed the highest sensitivity for IHC in mouse and human brain tissue, and clone 19H1K1 worked best in sandwich ELISAs using cell culture and (mouse) brain lysates. Although other clones such as 11H2K3 also performed quite well in MSD-ELISA and perhaps captured even better the peak intensities under more severe conditions (e.g., human AD brain tissue), clone 19H1K1 had a bigger assay window toward the lower

end of the signal. It appeared most useful to also detect the basal, physiological p-S65-Ub levels and subtle changes within cells, normal mouse brain, and human control brain. Whether differences in the sample matrix, changes in the Ub chain composition, or linkage preferences influenced the clones' overall performance in different applications or sample types remains to be determined. However, testing of the clones should be expanded to clinical biofluids in order to determine their full potential for also ultrasensitive detection of p-S65-Ub.

Here we capitalized on recent technological developments in the field and generated first recombinant, rabbit monoclonal antibodies against the mitophagy tag p-S65-Ub. Compared to conventional monoclonal antibodies derived from hybridoma cells lines, recombinant antibodies are not susceptible to genetic drift, gene loss, or mutations. As such recombinant antibodies are more stable and better scalable with minimal variability in specificity and excellent batch-to-batch reproducibility. Antibodies may also be recloned into backbones from a different species or conjugated with other epitope tags or direct site-specific labeling. Overall, this could generate more flexibility and enhance their versatility across applications where the host species may be limiting their utility [31]. Given the known sequences of the heavy and light chain variable regions, recombinant antibodies can be further engineered. For instance, the variable regions could be modified to further modulate the affinity to different Ub linkages, making them more selective for a certain Ub chain type. It was of interest that clones 11H2K3 and 30H3K1 were located on one end, while clone 41H1K3 was located on the opposite end on the phylogenetic tree. It is however not clear whether there is a correlation between the distance and their binding preferences with regards to Ub chain linkages.

In summary, we here introduce and characterize novel recombinant p-S65-Ub antibodies that can now be further exploited by the field to better understand mechanisms and nature of the PINK1-PRKN mediated p-S65-Ub signaling in a range of applications as well as its underlying implication in various disease-associated conditions. Our study also highlights the biomarker potential of the mitophagy tag in various clinical and pathological specimens as a diagnostic and prognostic tool or for therapeutic assessment.

## Materials and methods

### *Peptide synthesis, rabbit immunization, and polyclonal antibody production*

Synthetic peptides and the polyclonal antibodies were manufactured by 21<sup>st</sup> Century Biochemicals, Marlborough, MA. Briefly, peptides were manufactured by Fmoc-based solid phase peptide synthesis, HPLC purified to > 90%, and conjugated via the cysteine thiol to a mixture of carrier proteins. Each peptide was covalently attached to Optimized Affinity Resin (21<sup>st</sup> Century Biochemicals) containing an extended spacer arm and a thiol-reactive moiety. All rabbit animal work was conducted at Pacific Immunology (San Diego, CA; NIH and USDA compliant). After an initial rabbit immunization and multiple boosts, the serum was collected at specific

intervals and analyzed by dot blots at 21<sup>st</sup> Century Biochemicals after which appropriate production bleeds were pooled. The serum then underwent two purification processes. Antibodies were first recovered by affinity purification using p-S65-Ub peptides covalently attached to Optimized Affinity Resin through a cysteine residue added to either the N or C terminus. A portion of the resulting antibodies were further subjected to an additional immunodepletion step with both the nonphosphorylated Ub peptides (Ub Ser-OH N-/C-terminus) and PRKN peptides (p-S65-PRKN control and Ser-OH65-PRKN control). Peptide affinity columns were incubated with serum, washed multiple times including a 0.5 M NaCl wash in phosphate buffer, and the antibodies eluted under acidic conditions. After dialysis against PBS (Invitrogen 14,190–235), the antibodies were stored in PBS with 50% glycerol.

### *PBMC isolation, B cell selection, screening, and recombinant antibody generation*

Following the final boost, 30 ml of rabbit peripheral blood was collected for PBMC isolation and sent to ImmunoPrecise Antibodies Ltd. In short, the whole blood from each animal was diluted one to one in serum free medium and subjected to a density separation medium, Lympholyte-Mammal (Cedarlane Laboratories, L5110). Following the manufacturer's protocol, the enriched PBMCs at the middle layer were carefully removed and washed twice in 1% BSA (VWR, 9048-45-8) in DMEM (Corning, 15–018-CV). The isolated PBMCs were then subjected to an antigen specific enrichment process as part of the ImmunoPrecise Antibodies Ltd. Proprietary B Cell Select platform and were diluted in growth medium for single B cell cultivation. On day 7, the supernatant of each single B cell well was screened for antigen specificity through direct ELISA for targeting full-length monomeric p-S65-Ub protein (Boston Biochem, U-102), free p-S65-Ub peptides 1 and 2 and BSA-conjugated p-S65-Ub peptides 1 and 2 (provided by 21<sup>st</sup> Century Biochemicals). Non-phosphorylated Ub protein (Boston Biochem, U-100 H), free non-phosphorylated, hydroxylated Ub peptides 1 and 2, free p-S65-PRKN peptide, and free hydroxylated p-S65-PRKN peptide (provided by 21<sup>st</sup> Century Biochemicals) were used as negative controls.

The top 48 performing B cells from the screening were assessed and selected for recombinant expression. Briefly, mRNA was isolated (Dynabeads; Invitrogen 61,006) from lysed B cell cultures and RT-PCR was performed for the conversion to cDNA, followed by amplification of targeted heavy and light chains using specific primer sets. Variable regions of G1 and kappa chains were separately ligated into expression vectors containing respective constant regions. Plasmids encoding both the antibody heavy chain and light chain, housed within an expression vector driven by the CMV promoter were co-transfected into HEK293 cells, which had been adapted for suspension culture in a serum-free medium. Following transfection using the polyethylenimine-mediated gene delivery method, the cells were allowed to incubate for a further six days, resulting in 47 single clones that were producing recombinant antibodies. Variable region sequences

of antigen specific antibodies were determined by analysis of samples submitted to Psomagen, MD, USA (Table S1; Fig. S2).

Sequences for the top five recombinant antibodies were sent to Abcam for production of purified recombinant antibodies and commercial distribution. The five top performing antibodies produced in the supernatant were captured by Protein A ligands, specifically binding to the constant region (Fc) of the IgG antibodies (CH2-CH3 region) as the final purification step. The three best clones 30H3K1 (Abcam, ab309155, 30H3/30K1), 19H1K1 (Abcam, ab314901, 19H1/19K1), and 41H1K3 (Abcam, ab314903, 41H1/41K3) for different applications as recommended in Table 3 are publicly available (<https://www.michaeljfox.org/research-tools-catalog>).

### Dot blots using peptides

In peptide dot blots, phosphorylated and non-phosphorylated Ub 13-mers with central Ser65 respective PRKN 12mers (Ser65 in 6<sup>th</sup> position) were used in decrements of 5 (left to right) starting with 25  $\mu$ M, 5  $\mu$ M, 1  $\mu$ M and 0.2  $\mu$ M concentrations on 0.2  $\mu$ m Nitrocellulose membrane (BioRad 10,484,059). Ub peptides 1 and 2 had identical peptide sequences but different N- and C-terminal linker residues e.g., 6-Aminohexanoic Acid. The membrane was placed between 2 sheets of filter paper (Whatman 1,001,917) and dried overnight. The next morning the membrane was rinsed in Tris-buffered saline (TBS; 50 mM Tris [Millipore, G48311], 150 mM NaCl [FisherScientific, BP358], pH 7.4) for ~10 seconds, blocked in 5% skim milk (Sysco 5,398,953) in TBS with 0.1% Tween 20 (Fisher BioReagents, BP337500; TBS-T) for 30 min at room temperature. Primary antibodies were then added in a concentration of 1  $\mu$ g/ml in 5% BSA (Boston BioProducts, p-753) in TBS-T and incubated for 2 h at room temperature. Membranes were subsequently washed four times for 5 min in TBS-T before secondary antibody (Jackson ImmunoResearch, 711-035-152, 1:15,000) was added for 1 h at room temperature in 5% skim milk. Membranes were washed five times for 10 min each in TBS-T and detected with Immobilon Western Chemiluminescent HRP Substrate (Millipore Sigma, WBKLS0500) on Pro Signal Blotting film (Genesee Scientific, 30-810 L).

### Generation of MEFs

The *pink1* KO mice were obtained from the Jackson Laboratories (RRID:IMSR\_JAX:017946). Experiments were conducted in accordance with the Animal Scientific Procedures Act (1986) and with the Directive 2010/63/EU of the European Parliament and of the Council on the protection of animals used for scientific purposes (2010, no. 63). MEFs were generated using E13.5 embryos. Embryos were separated from placenta and individually placed into a single dish with cold DPBS, no calcium, no magnesium (Gibco 14,190,094). After dissection of the head and all internal organs, embryo bodies were chopped with a spring scissor to mince the tissue of 1–2 mm in a Petri dish. A small piece of tail was collected for genotyping. Tissues were digested for 15 min at 37°C with

digestion medium (0.025% Trypsin-EDTA [Gibco 25,300,054]; 0.125 mg/mL DNase I [Merck 11,284,932,001] in HBSS [Gibco 14,025,050]). After enzymatic digestion, tissue dissociation was completed by pipette trituration and trypsin neutralized with 5 ml of culturing media (DMEM [Gibco 11,960–085]; 20% heat-inactivated fetal bovine serum [Gibco 10,500,064]; 1% penicillin-streptomycin [Gibco 15,140,122], 1% L-glutamine [Gibco 25,030,024]; 1X non-essential amino acid [Gibco 11,140–035], 1X sodium pyruvate [Gibco 11,360–039]). Then, dissociated tissues were centrifuged at 300  $\times$  g for 5 min and resuspend in 5 ml culturing media. Cell suspension was filtered using a 70- $\mu$ m cell strainer in order to remove any undigested tissue pieces or aggregates from the cells. Cells were seeded in 10-cm dishes, containing 10 ml of pre-warmed culturing media, and cultured at 37°C in a humidified incubator with 5% CO<sub>2</sub>. Media was changed every 5 days and cells split at 90% confluence. A detailed protocol describing the preparation of mouse embryonic fibroblasts has been reported [32].

### Cell culture and treatment

WT and *PINK1* KO HEK293E cells were previously described [16] and were cultured in Dulbecco's modified Eagle medium (Thermo Fisher 11,965,118) supplemented with 10% fetal bovine serum (Neurocomics, FBS001800112). Primary human dermal fibroblasts were collected from a homozygous *PINK1*<sup>Q456X</sup> carrier and a healthy relative to serve as negative CON [33]. All fibroblasts were cultured in Dulbecco's modified Eagle medium supplemented with 10% fetal bovine serum, 1% PenStrep (Thermo Fisher 15,140,122), and 1% non-essential amino acids (Thermo Fisher 11,140,050). WT and *pink1* KO MEF cells have been described previously [28]. MEFs were grown in Dulbecco's modified Eagle medium supplemented with 20% fetal bovine serum, sodium pyruvate (Fisher Scientific 11,360–070), non-essential amino acids, and PenStrep. All cells were grown at 37°C, 5% CO<sub>2</sub>:air in humidified atmosphere. To induce mitophagy, HEK293E cells, MEFs, and human dermal fibroblasts were treated with 20  $\mu$ M CCCP (Sigma-Aldrich, C2759) (HEK293E cells), 5  $\mu$ M valinomycin (Cayman Chemicals 10,009,152) (MEFs), or 2  $\mu$ M valinomycin (human dermal fibroblasts), respectively, for 24 h. DMSO (Sigma-Aldrich, D4540) was used as vehicle treatment for human dermal fibroblasts. In HEK293E cells and in MEFs, both WT and *PINK1/pink1* KO cells were treated with CCCP respective valinomycin.

### Western blotting

HEK293E cells and MEFs were lysed in RIPA buffer (50 mM Tris, pH 8.0, 150 mM NaCl, 1% NP-40 [United States Biological 19,628], 0.5% deoxycholate [Sigma-Aldrich, D6750], 0.1% SDS [Bio-Rad 1,610,302]) containing protease inhibitor cocktail and phosphatase inhibitors (Sigma-Aldrich 11,697,498,001 and 04906837001). Cell lysates were then cleared for 15 min, 4°C at 20,817  $\times$  g and protein concentrations were determined by BCA assay (Thermo Fisher 23,225). Cell lysates (30, 15, 7.5  $\mu$ g for HEK293E cells or 10, 5, 2.5  $\mu$ g for MEFs) were diluted in Laemmli

buffer (62.5 mM Tris, pH 6.8, 1.5% SDS, 8.33% glycerol [Fisher Scientific, BP2291], 1.5%  $\beta$ -mercaptoethanol [Sigma-Aldrich, M3148], 0.005% bromophenol blue [Sigma-Aldrich, B5525]) and subjected to SDS-PAGE using 8–16% Tris-glycine gels (Invitrogen, EC60485BOX). Proteins were transferred onto polyvinylidene fluoride membranes (Millipore, Immobilon PSQ, ISEQ00010 or PVH00010) and the membranes were then blocked for 1 h in 5% nonfat milk in TBS-T and incubated in primary antibodies overnight in 5% BSA in TBS-T at 4°C. 1  $\mu$ g/ml of recombinant antibodies and 0.2  $\mu$ g/ml of the reference antibody (Cell Signaling Technology 62,802) were used. GAPDH (Meridian Life Science, H86504M, 0.025  $\mu$ g/ml) and VCL (vinculin) (Sigma, V9131, 0.016  $\mu$ g/ml) were used as loading controls. The following day, membranes were subjected to 1-h incubation with secondary antibodies (Jackson ImmunoResearch, 711-035-152 and 715-035-150) at room temperature. Proteins were visualized using Immobilon Western Chemiluminescent HRP Substrate (Millipore Sigma, WBKLS0500) on Pro Signal Blotting film (Genesee Scientific, 30-810 L) or on a Chemidoc MP imaging system (Bio-Rad, Hercules, CA, USA). Quantification of western blots was performed using Image Studio Lite software (LICOR Biosciences, Version 5.2). Intensity levels per area were background subtracted and normalized to the loading controls.

### **Tissue collection and preparation of mouse and human brain lysates**

A total of 12 WT and *pink1* KO mice ( $N = 3$  per sex/genotype) at age of three months were anesthetized and intracardially perfused with cold PBS. Brains were removed and immediately flash-frozen in liquid nitrogen. All animal procedures were in accordance with the ethical standards established by the Mayo Clinic and approved by the Institutional Animal Care and Use Committee at Mayo Clinic (A4649–19). Additionally, frozen human frontal cortex from ten AD and ten age- and sex-matched neurologically normal control cases were obtained from the Mayo Clinic Florida Brain Bank. All samples are from autopsies performed after approval by the legal next-of-kin. Research on de-identified postmortem brain tissue is considered exempt from human subjects' regulations by the Mayo Clinic Institutional Review Board.

For protein extraction, frozen brain tissues were homogenized in 5 $\times$  volumes of ice-cold RIPA buffer supplemented with protease and phosphatase inhibitors using glass Dounce tissue grinders (Fisher Scientific, K885300–0002). After 30 min incubation on ice, brain lysates were cleared by two times centrifugation at 20,000  $\times$  g, 4°C for 15 min. The resulting supernatant was collected as final lysates and protein concentrations were determined by BCA assay.

### **Sandwich MSD ELISA using recombinant protein, cell lysates, and tissue lysates**

Similar to the p-S65-Ub sandwich MSD ELISA that has been described previously [16], the top five recombinant p-S65-Ub antibodies or the reference antibody (Cell Signaling

Technology 62,802, E2J6T) were used as capturing agents. Detection was performed with a mouse Ub antibody (ThermoFisher, 14-6078-37, P4D1) followed by a Sulfo-tag labeled anti-mouse antibody (MSD, R32AC–1). All capturing antibodies were used at a concentration of 1  $\mu$ g/ml in 200 mM sodium carbonate buffer pH 9.7 and coated overnight at 4°C with 30  $\mu$ l per well in 96-well MSD plate (MSD, L15XA–3). The next morning MSD plates were washed two times with TBS-T and incubated with 300  $\mu$ l filtered blocking buffer (150 mM Tris, pH 7.4, 150 mM NaCl, 0.1% Tween-20, 1% BSA) for 1 h at 22°C. Antigen incubation was performed for 2 h at room temperature at 600 rpm on a microplate mixer (USA Scientific, 8182–2019). After washing, 30  $\mu$ l of detecting mouse Ub antibody (ThermoFisher, 14-6078-37, P4D1, 5  $\mu$ g/ml) were added to each well and incubated again for 2 h. 50  $\mu$ l Sulfo-tag labeled goat anti-mouse antibody (MSD, R32AC–1, 1:500) was next added and incubated for 1 h. The plates were then read on a MESO QuickPlex SQ 120 reader (Meso Scale Diagnostics, Rockville, MD, USA) after addition of 150  $\mu$ l MSD GOLD Read Buffer (MSD, R92TG–2).

For detection of recombinant proteins, K48 (Boston Biochem, UC-250) and K63 (Boston Biochem, UC-350) p-S65-Ub tetramers were serially diluted to a final concentration of 10 fg/ml to 1  $\mu$ g/ml. Their nonphosphorylated counterparts (Boston Biochem, UC-210b and UC-310b) were used as negative controls. For detection in HEK293E cell lysates, 10  $\mu$ g of protein was used with CCCP-treated *PINK1* KO cells serving as negative control and CCCP-treated WT cells serving as positive control. For detection in mouse and human brain lysates, 30  $\mu$ g of protein was used. All samples were run in duplicates and diluted in blocking buffer.

The LoB, LoD, and LoQ were calculated using MSD-ECL values from recombinant p-S65-Ub chains and according to *Armbruster and Pry* [19]. In brief, the LoBs were determined using the formula  $LoB = \text{mean}_{\text{blank}} + 1.645(\text{SD}_{\text{blank}})$  where blocking buffer served as blank. The LoD was determined using serial dilutions of p-S65-Ub analytes and calculated with the following formula:  $LoD = LoB + 1.645(\text{SD}_{\text{low concentration sample}})$ . The LoQ was determined as the lowest concentration of analyte that could be measured with a predefined goal for imprecision (here under 10%) or is clearly distinguishable from the LoB with more than 3 times the standard deviation.

### **Direct MSD ELISA using recombinant protein**

Recombinant p-S65-PRKN (Boston Biochem, E3–166), non-phosphorylated PRKN (Boston Biochem, E3–160) and p-S65-Ub monomer (Boston Biochem, U102) were initially dissolved in RIPA buffer (stock concentration of 1  $\mu$ g/ $\mu$ l), aliquoted in 1  $\mu$ l aliquots, flash-frozen in liquid nitrogen and stored at –80°C. Recombinant PRKN and p-S65-PRKN aliquots were serially (10-fold) diluted in 200 mM sodium carbonate buffer pH 9.7 with a starting concentration of 1  $\mu$ g/ml toward 10 fg/ml and used to coat the MSD plates overnight at 4°C without shaking with 50  $\mu$ l/well. Recombinant p-S65-Ub monomer (positive control) was used in equimolar concentration relative to the highest p-S65-PRKN concentration of

1 µg/ml. On the next morning, plates were washed twice with TBS-T and incubated for 1 h with blocking buffer without shaking at 22°C. Recombinant p-S65-Ub antibodies and the reference antibody in blocking buffer were subsequently incubated at a concentration of 1 µg/ml with 30 µl/well for 2 h at room temperature at 600 rpm on a microplate mixer. Fifty µl Sulfo-tag labeled goat anti-rabbit Ab (MSD, R32AB-1, 1:500) was next added and incubated for 1 h. The plates were then read on a MESO QuickPlex SQ 120 reader after addition of 150 µl MSD GOLD Read Buffer.

### **Immunofluorescence staining of fibroblasts followed by high content imaging**

To evaluate top clones for ICC and quantify p-S65-Ub levels using automated high-content imaging, WT and homozygous *PINK1*<sup>Q456X</sup> mutant fibroblasts were seeded in 96-well imaging plates (Fisher Scientific 08,772,225) and allowed to attach overnight. Cells were treated for 2 µM valinomycin (Enzo Life Science, BML-KC140-0025) or vehicle DMSO (Sigma-Aldrich, D4540) for 24 h and then fixed in 4% paraformaldehyde (Sigma-Aldrich 441,244) after one wash with PBS. Fibroblasts were immunostained with all clones or reference antibody against p-S65-Ub (Cell Signaling Technology 62,802, E2J6T) at 1 µg/ml and with HSPD1/HSP60 (arigo Biolaboratories, ARG10757, 1:2,000) followed by incubation with secondary antibody (Invitrogen, A-11034 and A-11041; 1:1,000) and Hoechst 33,342 (Invitrogen, H21492; 1:5,000). Plates were imaged using an Operetta CLS High Content imaging system (Perkin Elmer, Waltham, MA, USA) with a 20× water immersion objective using a 2 × 2 montage (no gaps) per well. Raw images were processed using the built-in Harmony analysis software to calculate the average cytoplasmic p-S65-Ub intensity per cell in each well.

### **Processing of fixed mouse and human tissue and immunohistochemistry**

Without doxycycline administration, rTg4510 mice used here constitutively express high levels of human P301L MAPT/tau in the hippocampus. Brain tissue from two nonTg and three rTg4510 transgenic mice at 9 months of age were used for IHC. All procedures were in accordance with the ethical standards established by the Mayo Clinic and approved by the Institutional Animal Care and Use Committee at Mayo Clinic (A15610). Additionally, autopsy brain from three AD cases were retrieved for IHC from the Mayo Clinic Florida Brain Bank. Research on de-identified postmortem brain tissue is considered exempt from human subjects' regulations by the Mayo Clinic Institutional Review Board.

Paraffin-embedded mouse hemibrain and human hippocampal tissue was cut into 5-µm serial sections and allowed to dry overnight at 60°C. Slides were deparaffinized and rehydrated, followed by antigen retrieval in steaming deionized water for 30 min. After blocking with 0.03% hydrogen peroxide (Sigma 216,763) and 5% normal goat serum (Invitrogen 16,210,072), serial sections from the same brain were incubated with all five clones, reference p-S65-Ub antibody (Cell Signaling Technology 62,802, E2J6T), or in-house p-S65-Ub antibody at 1.56 µg/ml (in

mouse brain) or 0.78 µg/ml (in human brain), followed by rabbit-labeled polymer HRP (Agilent, K4011) at room temperature. Independent sections from additional rTg4510 mice or human AD cases were processed similarly and stained with clone 41H1K3 at a concentration of 1.56 µg/ml or 0.125 µg/ml, respectively. Peroxidase labeling was visualized with the chromogen solution 3,3'-diaminobenzidine (Agilent, K4011). The sections were then counterstained with Lerner 1 hematoxylin (Fisher Scientific, CS400-1D) and coverslipped with Cytoseal mounting medium (Thermo Scientific, 8310). After IHC staining, all sections were imaged with an Aperio AT2 digital pathology scanner at 40 × magnification (Leica Biosystems, Wetzlar, Germany).

### **Statistical analysis**

Data analysis was performed in GraphPad Prism version 9 software. Unpaired t-test and Mann-Whitney U test were used for mouse and human brain ELISA analysis, respectively.

### **Acknowledgements**

We thank The Michael J. Fox Foundation for Parkinson's Research for their guidance and leadership in this collaborative effort. We are also grateful to the patients and their families who made this study possible. We thank the Center for Regenerative Medicine and the Neuroregeneration Laboratory for biobanking of patient cells at Mayo Clinic Florida. We also thank the Neuropathology Laboratory at Mayo Clinic Florida for processing mouse and human autopsy brain tissue and the excellent technical support.

### **Disclosure statement**

Mayo Clinic, F.C.F., and W.S. hold a patent related to PRKN activators (Small Molecule Activators of Parkin Enzyme Function, US patent, 11401255B2; August 02, 2022). Additional funding sources to disclose but not pertinent to the current study include a grant from Amazentis SA (to W.S.). Z.K.W. serves as PI or Co-PI on projects/grants from Biohaven Pharmaceuticals, Inc. and Vigil Neuroscience, Inc., and is an external advisory board member for Vigil Neuroscience, Inc., and a consultant on neurodegenerative medical research for Eli Lilly & Company. M.M.K.M. is a member of the Scientific Advisory Board of Montara Therapeutics Inc and scientific consultant to Merck Sharp and Dohme. J.B.F. was CEO at 21st Century Biochemicals Inc., K.P. is an employee of ImmunoPrecise Antibodies Ltd., and R.K. is an employee of Abcam Plc. All other authors declare they have no competing interests. This research was conducted in compliance with Mayo Clinic conflict of interest policies.

### **Funding**

This study was supported through grants from the Michael J. Fox Foundation for Parkinson's Research (017399 to W.S., 017367 to J.B.F., 017367.01 to K.P., and 022155 to R.K.). Work in the authors labs is further funded by the National Institute of Neurological Disorders and Stroke (NINDS: RF1 NS085070, R01 NS110085, and U54 NS110435 to W.S.), the National Institute on Aging (NIA: R56 AG062556 to W.S.), the Department of Defense Congressionally Directed Medical Research Programs (CDMRP) (W81XWH-17-1-0248 to W.S.), the Florida Department of Health - Ed and Ethel Moore Alzheimer's Disease Research Program (9AZ10 to W.S. and 22A07 to F.C.F.), the Ted Nash Long Life Foundation (W.S.) and The Michael J. Fox Foundation for Parkinson's Research (019046, 019258, and 021186 to W.S. and 021182 to F.C.F.). W.S. is also supported by Mayo Clinic Foundation, Mayo Clinic Center for Biomedical Discovery (CBD), and Mayo Clinic Robert



and Arlene Kogod Center on Aging. F.C.F. is further supported by Mayo Clinic Center for Biomedical Discovery (CBD), a Gerstner Family Career Development Award from the Mayo Clinic Center for Individualized Medicine (CIM), and the Mayo Clinic Younkin Scholar Program. X.H. is supported by Mayo Clinic Alzheimer Disease Research Center (ADRC, P30 AG062677) pilot and developmental project grants and research fellowships from the American Parkinson Disease Association (APDA) and the Alzheimer's Association (AARF-22-973152). Mayo Clinic Florida is an American Parkinson Disease Association (APDA) Center for Advanced Research (W.S., F.C.F., Z.K.W., and D.W.D.). Z.K.W. is partially supported by the National Institute of Aging (U19 AG063911), Mayo Clinic Center for Regenerative Medicine (CRM), gifts from the Donald G. and Jodi P. Heeringa Family, the Haworth Family Professorship in Neurodegenerative Diseases fund, the Albertson Parkinson's Research Foundation, and the PPNF Family Foundation. This work was supported by a Wellcome Trust Senior Research Fellowship in Clinical Science (210753/Z/18/Z to M.M.K.M.) and the Michael J. Fox Foundation (M.M.K.M.).

## Data availability statement

Access to the datasets used and/or analyzed during the current study are available from the corresponding author Dr. Wolfdieter Springer (Springer.Wolfdieter@mayo.edu) on request.

## ORCID

Jens O. Watzlawik  <http://orcid.org/0000-0003-0610-0267>  
 Xu Hou  <http://orcid.org/0000-0003-3011-4378>  
 Fabienne C. Fiesel  <http://orcid.org/0000-0002-1919-9676>  
 Wolfdieter Springer  <http://orcid.org/0000-0002-1178-3149>

## References

- Tanaka K. The PINK1–Parkin axis: an overview. *Neurosci Res.* 2020 Oct;159:9–15. doi: [10.1016/j.neures.2020.01.006](https://doi.org/10.1016/j.neures.2020.01.006)
- Lazarou M, Jin SM, Kane LA, et al. Role of PINK1 binding to the TOM complex and alternate intracellular membranes in recruitment and activation of the E3 ligase Parkin. *Dev Cell.* 2012 Feb 14;22(2):320–333. doi: [10.1016/j.devcel.2011.12.014](https://doi.org/10.1016/j.devcel.2011.12.014)
- Okatsu K, Uno M, Koyano F, et al. A dimeric PINK1-containing complex on depolarized mitochondria stimulates Parkin recruitment. *J Biol Chem.* [2013 Dec 20];288(51):36372–36384. doi: [10.1074/jbc.M113.509653](https://doi.org/10.1074/jbc.M113.509653)
- Kane LA, Lazarou M, Fogel AI, et al. PINK1 phosphorylates ubiquitin to activate Parkin E3 ubiquitin ligase activity. *J Cell Bio.* [2014 Apr 28];205(2):143–153. doi: [10.1083/jcb.201402104](https://doi.org/10.1083/jcb.201402104)
- Kazlauskaite A, Kondapalli C, Gourlay R, et al. Parkin is activated by PINK1-dependent phosphorylation of ubiquitin at Ser65. *Biochem J.* [2014 May 15];460(1):127–139. doi: [10.1042/BJ20140334](https://doi.org/10.1042/BJ20140334)
- Koyano F, Okatsu K, Kosako H, et al. Ubiquitin is phosphorylated by PINK1 to activate parkin. *Nature.* [2014 Jun 5];510(7503):162–166. doi: [10.1038/nature13392](https://doi.org/10.1038/nature13392)
- Kondapalli C, Kazlauskaite A, Zhang N, et al. PINK1 is activated by mitochondrial membrane potential depolarization and stimulates Parkin E3 ligase activity by phosphorylating Serine 65. *Open Biol.* 2012 May;2(5):120080. doi: [10.1098/rsob.120080](https://doi.org/10.1098/rsob.120080)
- Shiba-Fukushima K, Imai Y, Yoshida S, et al. PINK1-mediated phosphorylation of the parkin ubiquitin-like domain primes mitochondrial translocation of parkin and regulates mitophagy. *Sci Rep.* 2012;2(1):1002. doi: [10.1038/srep01002](https://doi.org/10.1038/srep01002)
- Ordureau A, Sarraf SA, Duda DM, et al. Quantitative proteomics reveal a feedforward mechanism for mitochondrial PARKIN translocation and ubiquitin chain synthesis. *Mol Cell.* [2014 Nov 6];56(3):360–375. doi: [10.1016/j.molcel.2014.09.007](https://doi.org/10.1016/j.molcel.2014.09.007)
- Wauer T, Simicek M, Schubert A, et al. Mechanism of phospho-ubiquitin-induced PARKIN activation. *Nature.* [2015 Aug 20];524(7565):370–374. doi: [10.1038/nature14879](https://doi.org/10.1038/nature14879)
- Zheng X, Hunter T. Pink1, the first ubiquitin kinase. *Embo J.* [2014 Aug 1];33(15):1621–1623. doi: [10.15252/emboj.201489185](https://doi.org/10.15252/emboj.201489185)
- Ding WX, Yin XM. Mitophagy: mechanisms, pathophysiological roles, and analysis. *Biol Chem.* 2012 Jul;393(7):547–564. doi: [10.1515/hsz-2012-0119](https://doi.org/10.1515/hsz-2012-0119)
- Amorim JA, Coppotelli G, Rolo AP, et al. Mitochondrial and metabolic dysfunction in ageing and age-related diseases. *Nat Rev Endocrinol.* 2022 Apr;18(4):243–258. doi: [10.1038/s41574-021-00626-7](https://doi.org/10.1038/s41574-021-00626-7)
- Hou X, Fiesel FC, Truban D, et al. Age- and disease-dependent increase of the mitophagy marker phospho-ubiquitin in normal aging and lewy body disease. *Autophagy.* 2018;14(8):1404–1418. doi: [10.1080/15548627.2018.1461294](https://doi.org/10.1080/15548627.2018.1461294)
- Watzlawik JO, Fiesel FC, Fiorino G, et al. Basal activity of PINK1 and PRKN in cell models and rodent brain. *Autophagy.* 2023 Dec;2:1–12. doi: [10.1080/15548627.2023.2286414](https://doi.org/10.1080/15548627.2023.2286414) Online ahead of print.
- Watzlawik JO, Hou X, Fricova D, et al. Sensitive ELISA-based detection method for the mitophagy marker p-S65-Ub in human cells, autopsy brain, and blood samples. *Autophagy.* 2021 Sep;17(9):2613–2628. doi: [10.1080/15548627.2020.1834712](https://doi.org/10.1080/15548627.2020.1834712)
- Fiesel FC, Ando M, Hudec R, et al. (Patho-)physiological relevance of PINK1-dependent ubiquitin phosphorylation. *EMBO Rep.* 2015 Sep;16(9):1114–1130. doi: [10.15252/embr.201540514](https://doi.org/10.15252/embr.201540514)
- Hou X, Watzlawik JO, Cook C, et al. Mitophagy alterations in Alzheimer's disease are associated with granulovacuolar degeneration and early tau pathology. *Alzheimer's & Dementia.* [2020 Oct 8];17(3):417–430. doi: [10.1002/alz.12198](https://doi.org/10.1002/alz.12198)
- Armbruster DA, Pry T. Limit of blank, limit of detection and limit of quantitation. *Clin Biochem Rev.* 2008 Aug;29(Suppl 1):S49–52.
- Fiesel FC, Springer W. Disease relevance of phosphorylated ubiquitin (p-S65-Ub). *Autophagy.* [2015 Nov 2];11(11):2125–2126. doi: [10.1080/15548627.2015.1091912](https://doi.org/10.1080/15548627.2015.1091912)
- Shiba-Fukushima K, Ishikawa KI, Inoshita T, et al. Evidence that phosphorylated ubiquitin signaling is involved in the etiology of Parkinson's disease. *Hum Mol Genet.* [2017 Aug 15];26(16):3172–3185. doi: [10.1093/hmg/ddx201](https://doi.org/10.1093/hmg/ddx201)
- Potting C, Crochemore C, Moretti F, et al. Genome-wide CRISPR screen for PARKIN regulators reveals transcriptional repression as a determinant of mitophagy. *Proc Natl Acad Sci U S A.* [2018 Jan 9];115(2):E180–E189. doi: [10.1073/pnas.1711023115](https://doi.org/10.1073/pnas.1711023115)
- Soutar MPM, Melandri D, O'Callaghan B, et al. Regulation of mitophagy by the NSL complex underlies genetic risk for Parkinson's disease at 16q11.2 and MAPT H1 loci. *Brain.* [2022 Dec 19];145(12):4349–4367. doi: [10.1093/brain/awac325](https://doi.org/10.1093/brain/awac325)
- Hou X, Heckman MG, Fiesel FC, et al. Genome-wide association study identifies APOE and ZMIZ1 variants as mitophagy modifiers in Lewy body disease. *medRxiv.* [2023 Oct 16. doi: [10.1101/2023.10.16.23297100](https://doi.org/10.1101/2023.10.16.23297100).
- Chin RM, Rakhit R, Ditsworth D, et al. Pharmacological PINK1 activation ameliorates pathology in Parkinson's disease models. *bioRxiv.* [2023 Feb 15]. doi: [10.1101/2023.02.14.528378](https://doi.org/10.1101/2023.02.14.528378)
- Hou X, Chen TH, Koga S, et al. Alpha-synuclein-associated changes in PINK1-PRKN-mediated mitophagy are disease context dependent. *Brain Pathol.* 2023 Sep;33(5):e13175. doi: [10.1111/bpa.13175](https://doi.org/10.1111/bpa.13175)
- Swatek KN, Usher JL, Kueck AF, et al. Insights into ubiquitin chain architecture using Ub-clipping. *Nature.* 2019 Aug;572(7770):533–537. doi: [10.1038/s41586-019-1482-y](https://doi.org/10.1038/s41586-019-1482-y)
- Antico O, Ordureau A, Stevens M, et al. Global ubiquitylation analysis of mitochondria in primary neurons identifies endogenous Parkin targets following activation of PINK1. *Sci Adv.* [2021 Nov 12];7(46):eabj0722. doi: [10.1126/sciadv.abj0722](https://doi.org/10.1126/sciadv.abj0722)
- Ordureau A, Paulo JA, Zhang W, et al. Dynamics of PARKIN-dependent mitochondrial ubiquitylation in induced neurons and model systems revealed by digital snapshot

- proteomics. *Mol Cell*. [2018 Apr 19];70(2):211–227 e8. doi: [10.1016/j.molcel.2018.03.012](https://doi.org/10.1016/j.molcel.2018.03.012)
- [30] Deol KK, Strieter ER. The ubiquitin proteoform problem. *Curr Opin Chem Biol*. 2021 Aug;63:95–104. doi: [10.1016/j.cbpa.2021.02.015](https://doi.org/10.1016/j.cbpa.2021.02.015)
- [31] Trimmer JS. Recombinant antibodies in basic neuroscience research. *Curr Protoc Neurosci*. 2020 Dec;94(1):e106. doi: [10.1002/cpns.106](https://doi.org/10.1002/cpns.106)
- [32] Antico O, Ordureau A, Stevens M, et al. Reconstitution of Parkin ubiquitin ligase activity using mouse and human mitochondria. *protocols.io*. 2021. doi:[10.17504/protocols.io.bxmypk7w](https://doi.org/10.17504/protocols.io.bxmypk7w)
- [33] Siuda J, Jasinska-Myga B, Boczarska-Jedynak M, et al. Early-onset Parkinson's disease due to PINK1 p.Q456X mutation—clinical and functional study. *Parkinsonism Relat Disord*. 2014 Nov;20(11):1274–1278. doi: [10.1016/j.parkreldis.2014.08.019](https://doi.org/10.1016/j.parkreldis.2014.08.019)